A variational formulation of crack phase-field modeling for ductile fracture equipped two damage variables

Jike HAN, Tohoku University
Seishiro MATSUBARA, Nagoya University
Shuji Moriguchi, Tohoku University
Kenjiro TERADA, Tohoku University
E-mail: han.jike.s7@dc.tohoku.ac.jp

This study presents a variational formulation of crack phase-field modeling for ductile fracture. Constitutive work density consists of elastic, plastic, and crack components, with damage variables separately introduced for elasticity and plasticity. The proposed model is equipped with thresholds and coefficients to control the amount of damage driving force, while variational consistent evolution laws for damage are derived as stationary conditions from a supremum problem of dissipative potential. Also, governing equations are derived from an optimization problem within the continuum thermodynamics framework. The characteristic features of the proposed model are demonstrated with numerical examples.

1. Introduction

Crack phase-field model[1)] (PF model) has received attention due to its capability to predict arbitrary crack propagation and its compatibility with classical fracture mechanics. This study presents a variational formulation for ductile fracture equipped with two damage variables for elasticity and plasticity. The proposed model is equipped with thresholds and coefficients to control the amount of damage driving force, while damage evolution laws follow a variational structure.

2. Proposed model

2.1. Constitutive work density functional

In line with our previous study[2)], we define the following constitutive work density functional:

$$\Psi = \Psi^{\mathrm{e}} + \Psi^{\mathrm{p}} + \Psi^{\mathrm{f}}, \tag{1}$$

where Ψ^{e}, Ψ^{p}, and Ψ^{f} denote the elastic and plastic strain energy densities and the energy density due to crack surface generation, respectively. The elastic part follows a tensile-compressive split as

$$\Psi^{\mathrm{e}} = g\left(d^{\mathrm{e}}\right)\Psi_0^{\mathrm{e}+} + \Psi_0^{\mathrm{e}-}, \tag{2}$$

where $\Psi_0^{\mathrm{e}+}$ and $\Psi_0^{\mathrm{e}-}$ denote the effective tensile and compressive amounts of Ψ^{e}. Note that the reduction of material stiffness is considered by the degradation function $g\left(d^{\mathrm{e}}\right)$, which is determined by the elastic damage variable d^{e}. Similarly, the plastic part is defined as

$$\Psi^{\mathrm{p}} = g\left(d^{\mathrm{p}}\right)\Psi_0^{\mathrm{p}}, \tag{3}$$

where Ψ_0^{p} denotes the effective amount of Ψ^{p}. Also, another degradation function, which is determined by the plastic damage variable d^{p}, is introduced. Here, d^{p} does not directly contribute to the deterioration of material but affects the evolution of plastic hardening variable. In addition, the energy density due to crack surface generation is defined as

$$\Psi^{\mathrm{f}} := \int_0^t G_{\mathrm{c}}\left(\boldsymbol{F}^{\mathrm{e}}, \alpha\right)\gamma_{l_{\mathrm{f}}}\, dt, \tag{4}$$

where $G_{\mathrm{c}}\left(\boldsymbol{F}^{\mathrm{e}}, \alpha\right)$ and $\gamma_{l_{\mathrm{f}}}$ denote the degrading fracture toughness and the crack surface density. Note that G_{c} is degraded by the accumulation of plastic strain and the increase of mean stress, which reflects the effect of stress triaxiality. Also, since G_{c} has a process-dependent property, we have defined Ψ^{f} as a time-dependent format.

2.2. Evolution laws for plasticity and damage

The energy dissipation of the proposed model is given as

$$\mathcal{D}^{\mathrm{pf}} = \boldsymbol{\tau} : \boldsymbol{d}^{\mathrm{p}} - r^{\mathrm{p}}\dot{\alpha} + \tau^{\mathrm{fe}}\dot{d}^{\mathrm{e}} + \tau^{\mathrm{fp}}\dot{d}^{\mathrm{p}} - r^{\mathrm{f}}\dot{d}, \tag{5}$$

where $\boldsymbol{\tau}$, r^{p}, τ^{fe}, τ^{fp} and r^{f} are the driving force of plasticity, plastic dissipative resistance force, elastic driving force and plastic driving forces, and damage dissipative resistance force. Then, let us define the following supremum problem of the dissipative potential density based on the maximum dissipation principle:

$$\mathcal{V}^{\mathrm{pf}} = \sup_{[\boldsymbol{\tau}_{\mathrm{dev}}, r^{\mathrm{p}}, \tau^{\mathrm{fe}}, \tau^{\mathrm{fp}}, r^{\mathrm{f}}]} \sup_{[\lambda^{\mathrm{p}}, \lambda^{\mathrm{f}}]} \underbrace{\mathcal{D}^{\mathrm{pf}} - \lambda^{\mathrm{p}}\Phi^{\mathrm{p}} - \lambda^{\mathrm{f}}\Phi^{\mathrm{f}}}_{\tilde{\mathcal{V}}^{\mathrm{pf}}}, \tag{6}$$

where we have introduced two threshold functions to prescribe the admissible stress fields with respect to plasticity and damage. Their specific forms are as follows:

$$\begin{aligned}
\Phi^{\mathrm{p}} &:= \frac{||\boldsymbol{\tau}_{\mathrm{dev}}||}{g\left(d^{\mathrm{e}}\right)} - \sqrt{\frac{2}{3}}\frac{r^{\mathrm{p}}}{g\left(d^{\mathrm{p}}\right)} \\
\Phi^{\mathrm{f}} &:= \tau^{\mathrm{fe}*} + \tau^{\mathrm{fp}*} - r^{\mathrm{f}} \\
\text{with}\quad & \tau^{\mathrm{fe}*} = -\partial_{d^{\mathrm{e}}} g\left(d^{\mathrm{e}}\right)\langle\Psi_0^{\mathrm{e}+} - \Psi_{\mathrm{cr}}^{\mathrm{e}}\rangle\zeta^{\mathrm{e}} \\
& \tau^{\mathrm{fp}*} = -\partial_{d^{\mathrm{p}}} g\left(d^{\mathrm{p}}\right)\langle\Psi_0^{\mathrm{p}} - \Psi_{\mathrm{cr}}^{\mathrm{p}}\rangle\zeta^{\mathrm{p}}.
\end{aligned} \tag{7}$$

where $\tau^{\mathrm{fe}*}$ and $\tau^{\mathrm{fp}*}$ are the "modified" elastic and plastic driving forces along with the conditions $\tau^{\mathrm{fe}*} \leq \tau^{\mathrm{fe}}$ and $\tau^{\mathrm{fp}*} \leq \tau^{\mathrm{fp}}$. Also, two threshold parameters $\Psi_{\mathrm{cr}}^{\mathrm{e}}$ and $\Psi_{\mathrm{cr}}^{\mathrm{p}}$ and coefficients $\zeta^{\mathrm{e}} \in [0,1]$ and $\zeta^{\mathrm{p}} \in [0,1]$ have been introduced to control the contributions of elastic and plastic strain energies for damage evolution. We impose the stationary conditions of Eq. (6) with respect to the involved primary variables to derive the five evolution laws accompanied by the following corresponding loading/unloading conditions:

$$\left\{\begin{aligned}
\boldsymbol{d}^{\mathrm{p}} &= \frac{\lambda^{\mathrm{p}}}{g\left(d^{\mathrm{e}}\right)}\frac{\boldsymbol{\tau}_{\mathrm{dev}}}{||\boldsymbol{\tau}_{\mathrm{dev}}||} \\
\dot{\alpha} &= \sqrt{\frac{2}{3}}\frac{\lambda^{\mathrm{p}}}{g\left(d^{\mathrm{p}}\right)} \\
\dot{d}^{\mathrm{e}} &= \lambda^{\mathrm{f}}\zeta^{\mathrm{e}}\chi^{\mathrm{e}} \\
\dot{d}^{\mathrm{p}} &= \lambda^{\mathrm{f}}\zeta^{\mathrm{p}}\chi^{\mathrm{p}} \\
\dot{d} &= \lambda^{\mathrm{f}}
\end{aligned}\right., \quad \left\{\begin{aligned}
&\lambda^{\mathrm{p}} \geq 0,\ \Phi^{\mathrm{p}} \leq 0,\ \lambda^{\mathrm{p}}\Phi^{\mathrm{p}} = 0 \\
&\lambda^{\mathrm{f}} \geq 0,\ \Phi^{\mathrm{f}} \leq 0,\ \lambda^{\mathrm{f}}\Phi^{\mathrm{f}} = 0
\end{aligned}\right., \tag{8}$$

in which χ^{e} and χ^{p} are step functions defined as

$$\chi^{\mathrm{e}} = \begin{cases} 1 & \text{if } \Psi_0^{\mathrm{e}+} - \Psi_{\mathrm{cr}}^{\mathrm{e}} > 0 \\ 0 & \text{otherwise} \end{cases}, \quad \chi^{\mathrm{p}} = \begin{cases} 1 & \text{if } \Psi_0^{\mathrm{p}} - \Psi_{\mathrm{cr}}^{\mathrm{p}} > 0 \\ 0 & \text{otherwise} \end{cases}. \tag{9}$$

©公益社団法人土木学会 応用力学委員会

2.3. Global governing equations

The stationary conditions of the total rate potential, which is defined by Ψ, $\mathcal{V}^{\mathrm{pf}}$, and external forces, yield the following global governing equations:

• Equilibrium for mechanical field:

$$\frac{\partial}{\partial \boldsymbol{X}} \cdot \boldsymbol{P} + \boldsymbol{B} = \boldsymbol{0}, \quad \text{Neumann cond. } \boldsymbol{P} \cdot \boldsymbol{N} = \boldsymbol{T}, \tag{10}$$

• Equilibrium for micromorphic plastic field:

$$\frac{\partial \Psi^{\mathrm{p}}}{\partial \alpha} - \frac{d}{d\boldsymbol{X}} \cdot \frac{\partial \Psi^{\mathrm{p}}}{\partial \nabla \alpha} = 0, \quad \text{Neumann cond. } \nabla \alpha \cdot \boldsymbol{N} = 0, \tag{11}$$

• Equilibrium for phase-field:

$$r^{\mathrm{f}} = \frac{\partial \Psi^{\mathrm{f}}}{\partial d} - \frac{d}{d\boldsymbol{X}} \cdot \frac{\partial \Psi^{\mathrm{f}}}{\partial \nabla d}, \quad \text{Neumann cond. } \nabla d \cdot \boldsymbol{N} = 0, \tag{12}$$

• Plastic force / Hardening force:

$$\boldsymbol{\tau} = 2 \frac{\partial \Psi^{\mathrm{e}}}{\partial \boldsymbol{b}^{\mathrm{e}}} \cdot \boldsymbol{b}^{\mathrm{e}}, \quad r^{\mathrm{p}} = \frac{\partial \Psi^{\mathrm{p}}}{\partial \bar{\alpha}}, \tag{13}$$

• Elastic / Plastic damage driving force:

$$\tau^{\mathrm{fe}} = -\frac{\partial \Psi^{\mathrm{e}}}{\partial d^{\mathrm{e}}}, \quad \tau^{\mathrm{fp}} = -\frac{\partial \Psi^{\mathrm{p}}}{\partial d^{\mathrm{p}}}, \tag{14}$$

3. Numerical example

This numerical example is devoted to the demonstration of the crack representation performance using the proposed model. Tensile failures for the two-dimensional symmetrically notched specimen are considered, as shown in Fig. 1. The Swift hardening function $\hat{y}(\bar{\alpha}) = y_{\mathrm{a}}(\bar{\alpha} + \alpha_{\mathrm{b}})^{\beta_{\mathrm{c}}}$ is used for the hardening behavior of plastic deformation. The material properties and other parameters for damage computation are provided in Table 1.

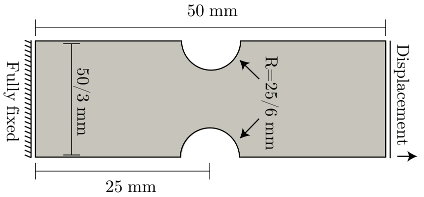

Fig. 1 Geometry and boundary conditions for the specimen.

Table 1 Material parameters for the specimen.

Parameter		Value	Unit
Young's modulus	E	200000	[MPa]
Poisson's ratio	ν	0.3	[-]
Strength coefficient	y_{a}	1169	[MPa]
Pre-strain parameter	α_{b}	0.0033	[-]
Hardening parameter	β_{c}	0.1	[-]
Plastic length scale parameter	l_{p}	0.2	[mm]
Penalty parameter	p_{p}	2500	[MPa]
Initial fracture toughness	G_{c0}	1000	[N/mm]
Critical fracture toughness	$G_{\mathrm{c}\infty}$	10	[N/mm]
Degradation threshold	α_{cr}	0	[-]
Crack length scale parameter	l_{f}	0.2	[mm]
Elastic damage coefficient	ζ^{e}	1.0	[-]
Elastic damage threshold	$\Psi^{\mathrm{e}}_{\mathrm{cr}}$	0	[MPa]

Seven cases with different combinations of parameters relating to damage evolution are investigated. Because of space limitaion, we show the load-displacement curves for the cases IV, V, VI, and VII only in Fig. 2 and the damage distributions for the cases IV and VI Fig. 3, respectively. As shown in Fig. 2, cases IV and V exhibit stress drop after relatively large deformation, while cases VI and VII show relatively small deformation. Specifically, a slanted crack path is obtained in case IV. This is due to the fact that the crack initiates along with the shear band. Meanwhile, the almost horizontal crack pattern is obtained for case VI. That is, the crack initiates from both notch surfaces towards the center of the specimen. This is because the accumulation of plastic strain is concentrated on the notch tips in the early plastic deformation state. Note that similar crack patterns are seen in previous studies[3,4], and the proposed model is thus unified in nature and is able to mimic the existing PF models by adjusting the parameters related to damage.

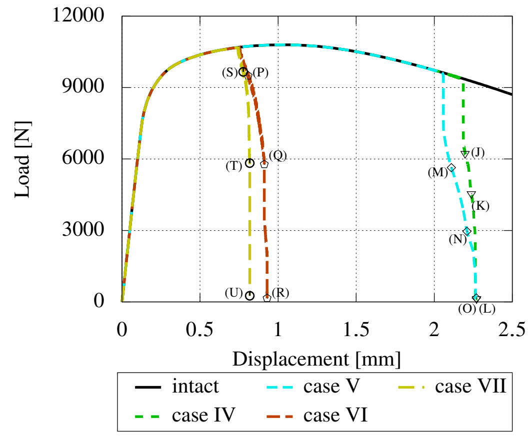

Fig. 2 Load-displacement curves for the specimen.

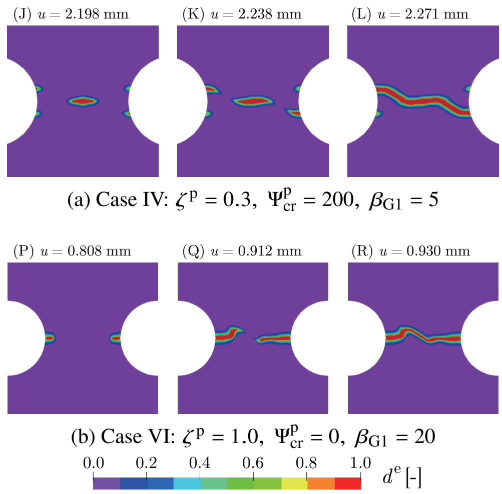

(a) Case IV: $\zeta^{\mathrm{p}} = 0.3$, $\Psi^{\mathrm{p}}_{\mathrm{cr}} = 200$, $\beta_{\mathrm{G1}} = 5$

(b) Case VI: $\zeta^{\mathrm{p}} = 1.0$, $\Psi^{\mathrm{p}}_{\mathrm{cr}} = 0$, $\beta_{\mathrm{G1}} = 20$

Fig. 3 Crack evolutions for the specimen.

4. Conclusion

The crack phase-field model is known for its ability to predict the initiation of an arbitrary crack, its propagation, and bifurcation while remaining compatible with classical fracture mechanics. In this study, a variational formulation is carried out to derive evolution laws separately for plasticity and damage as the stationary conditions of the supremum problem of the dissipative potential. As a result, the proposed model involves two damage variables associated with the elastic and plastic driving forces in damage evolution. The characteristic features of the proposed model are demonstrated by presenting numerical examples.

References

1) Miehe et al. *Int. J. Numer. Methods Eng.* **83** (10), pp.1273–1311, 2010.
2) Han et al. *Comput. Mech.* **69** (1), pp.151–175, 2022.
3) Ambati et al. *Comput. Mech.* **55** (2), pp.383–405, 2015.
4) Yin & Kaliske *Comput. Methods in Appl. Mech. Eng.* **366**, pp.113068, 2020.

©公益社団法人土木学会 応用力学委員会